International Journal of Solids and Structures 49 (2012) 846–852

Contents lists available at SciVerse ScienceDirect

International Journal of Solids and Structures

journal homepage: www.elsevier.com/locate/ijsolstr

Theoretical approach of nanostructuration effects on surface energies

V. Raspal, K.O. Awitor *

C-BIOSENSS, Clermont Université, Université d'Auvergne, BP 10448, F-63000 Clermont-Ferrand, France

ARTICLE INFO

Article history:
Received 19 July 2011
Received in revised form 11 October 2011
Available online 19 December 2011

Keywords:
Surface energy
Nanoparticles
Nanostructured surfaces
van der Waals potential
Superpositional principle

ABSTRACT

The wettability control of the nanostructured surfaces requires the knowledge of the surface energy. In this work, van der Waals potential has been used to theoretically predict the surface energy of nanoparticles or nanostructured surfaces. The model predicts that, for length scales below 30 nm, a single sphere exhibits an over-energetic term while spheres arranged in a close-packed manner highlight a complex competition between the porosity and the intrinsic low-radius effect. All nanostructuration effects vanish for greater sizes. Above 30 nm, the surface energy tends to reach its classical value.

1. Introduction

Most implants in the living are still badly tolerated and cause infections and inflammation due to the living organism's response. In order to overcome this biological barrier, it is crucial to control the chemical and physical properties of the interface between the medical device and the host because most of the known problems definitely arise at this junction. In this work, van der Waals potential has been used to theoretically predict the surface energy of nanoparticles or nanostructured surfaces. Indeed, the nanostructures happen to possess many assets so they can, at least partially, aspire to be a solution for a better integration of implantable medical devices. For instance, it is possible to fabricate nanoporous surfaces which can potentially load and release drugs or other molecules of interest (Awitor et al., 2008; Robert-Goumet et al., 2009; Gultepe et al., 2010; Liang et al., 2011; Perry et al., 2011; Kwak et al., 2010; Aw et al., 2011). It should constitute a very well targeted treatment. The behavior of such nanostructured surfaces in relation to the living as well as drug diffusion mechanisms are not yet well known. The surface energy is one important key as well as the various possible surface topographies (nanopores, nanodots, nanopillars, etc.). By affecting the wettability, the surface energy controls the affinity between the device, the living environment and other molecules. The reference Yang and Leong (2010) gives an interesting rundown of techniques of great potential in regenerative medicine including vascular, bone, neural and stem cell tissue engineering. It has been observed that surface energy and topography can be decisive as far as a biological medium is concerned. One remarkable example of this field is the impact of the nanoscale environment on cell behavior. Park et al. (2007) and von Wilmowsky et al. (2011) went into it in depth. It was shown that a peri-implant bone growth was strongly affected by the diameter of TiO_2 nanotubes of the implant surface. Although the value of the surface energy of a material can be reached by different experiments, its evolution for a nanoparticle or a nanoasperity against the size is still very controversial. On the one hand, Bradley (1932), Derjaguin (1934), De Boer (1936) and Hamaker (1937) were the first to have computed the effective interaction between two macroscopic bodies in the vaccum based on van der Waals intermolecular interactions. On the other hand, Tolman (1948) was the first to have tried to theorize the effect of curvature of an interface on Gibbs free surface energy. After him, many experimenters followed the same goal based on thermodynamical considerations (Hill, 1950; Fisher and Wortis, 1984; Lei et al., 2005; Nishioka et al., 1989; Nanda, 2005). Statistical mechanics was also a means used for this estimation (Falls et al., 1981; Guermeur et al., 1985; Baidakov and Boltachev, 1999) as well as molecular dynamics (Nanda et al., 2003; Jia et al., 2009). Conclusions are often contradictory, involving for instance the sign of Tolman's length (Lei et al., 2005; Van Giessen et al., 1998). Some of them predict an increase of surface energy when the interface curvature gets greater (Moody and Attard, 2001) whereas others predict the contrary. Nishioka et al. (1989) evokes a surface energy 20% smaller for a curvature being about five intermolecular distances.

This paper also supports the hypothesis that the surface energy is modulated by the curvature of the interface when the scale is less than a few tens of nanometers. All surface free energies are computed based on the superpositional principle of the classical Hamaker–De Boer approach to the van der Waals interaction. For

* Corresponding author.
E-mail address: komla.awitor@u-clermont1.fr (K.O. Awitor).

0020-7683/$ - see front matter © 2011 Elsevier Ltd. All rights reserved.
doi:10.1016/j.ijsolstr.2011.12.003

this reason, the scope of this model is limited to neutral and apolar compounds and cannot apply to ionic systems or metals. Polar molecules are to be excluded from the field of this study because they involve correlations of dipole orientation so that interactions between them are never properly additive. Keesom and Debye interactions have to be negligible. Our model focuses on the surface energy of a particle itself. It is based on Hamaker's well known calculations (Hamaker, 1937) on the energy of two interacting particles. The paper begins with a reminder of the classical case of planar surfaces and gives the expression of surface energy in terms of the Hamaker constant and the intermolecular distance. This expression is then used as a yardstick. First, a single sphere is studied as a function of its radius. Then, the effect of a periodization pattern is studied. In both cases, a correction factor is defined in terms of some reduced characteristic quantities and then analyzed. The single sphere exhibits an over-energetic term as a result of the radius decrease. The periodization highlights a complex competition between the previous intrinsic low-radius effect and the porosity of the environment that tends to decrease surface energy. The scope of these results is broad because they may apply to both solid nanoparticles in vacuum as well as nanoasperities dug into a solid.

2. Quantities definition

$\mathcal{E}$	potential energy of van der Waals interaction between two bodies
$\mathcal{S}$	solid (an index designates one part of this solid after it was broken)
ρ	atomic density of a body
α	polarisability of a particle
V	solid volume
$\mathrm{d}\tau$	element of a solid volume
R	sphere radius
D	center-to-center distance between two neighboring spheres
a_0	intermolecular distance
W	potential energy of interaction per unit surface
γ	surface energy of a phase (solid or liquid)
A	Hamaker constant
C	London–van der Waals constant
ζ	correction factor of the surface energy of a given surface compared to a flat surface
i, **j**, **k**	basis vectors of an orthonormal basis
a, **b**, **c**	basis vectors of a hexagonal lattice
x	normalized sphere radius
y	normalized space between two spheres
r, r', l, d	generic lengths used as calculation intermediates

3. van der Waals interaction potential

van der Waals potential is universal and combines Keesom, Debye and London forces. It is responsible for the cohesion of neutral solids and liquids. For this reason, these forces have to be overcome to break a solid or a liquid and to create a new free surface. The van der Waals potential is a good candidate for the study of the origin and the evaluation of surface energies.

Let us consider two bodies which volumes are V_1 and V_2. Their respective atomic densities are noted ρ_1 and ρ_2. These two neutral bodies interact through a van der Waals potential. Assuming that two atoms experience the same interaction regardless of the presence of other atoms between them, a pairwise summation can be carried out over V_1 and V_2. The potential energy of the system is:

$$\mathcal{E} = -\int_{V_1} \mathrm{d}\tau_1 \int_{V_2} \mathrm{d}\tau_2 \frac{C_{12}\rho_1\rho_2}{r^6} \tag{1}$$

where r stands for the distance between elementary volumes $\mathrm{d}\tau_1$ and $\mathrm{d}\tau_2$. C_{12} is called London–van der Waals constant for the media 1 and 2, combining Keesom, Debye and London interaction constants and depending on respective polarisabilities α_1 and α_2 among others.

4. Flat surface: the classical case

The goal of this part consists of obtaining the expression of the surface energy γ of a solid surface. One must remember that the so-called surface energy is the work needed to create a free unit surface within the solid bulk. This paragraph is particularly focused on the classical case of a flat solid surface. The problem is to break an ideal infinite solid $\mathcal{S}$ along a plane and then to separate its two parts $\mathcal{S}_1$ and $\mathcal{S}_2$ far away from each other (an ideal infinite distance is necessary so that any interaction acting on them vanishes).

We start the process with the estimation of the potential energy associated with the interaction of $\mathcal{S}_1$ and an elementary volume from $\mathcal{S}_2$. To this end, $\mathcal{S}_1$ is divided into volumes $\mathrm{d}v_1$. Each of them is defined by a specific distance r to $\mathrm{d}\tau_2$ (see Fig. 1).

The elementary volume $\mathrm{d}v_1$ is expressed by:

$$\mathrm{d}v_1 = 2\pi r^2(1-\cos\theta)\mathrm{d}r \tag{2}$$

So, noting that $r' = r\cos\theta$ and applying the general expression of Eq. (1) leads to:

$$\mathrm{d}\mathcal{E} = -\frac{\pi C_{12}\rho_1\rho_2}{6r'^3}\mathrm{d}\tau_2 \tag{3}$$

Let us consider $\mathrm{d}\tau_2 = \mathrm{d}S\mathrm{d}r'$ where $\mathrm{d}S$ is one side of the elementary surface containing $\mathrm{d}\tau_2$, parallel to the surface $\mathcal{S}_2$. Potential energy per unit surface is W and is given by:

$$\mathrm{d}W = \frac{\mathrm{d}\mathcal{E}}{\mathrm{d}\tau_2}\mathrm{d}r' \tag{4}$$

$$W(\Lambda) = -\frac{\pi C_{12}\rho_1\rho_2}{6}\int_{\Lambda}^{\infty}\frac{\mathrm{d}r'}{r'^3} \tag{5}$$

$$W(\Lambda) = -\frac{\pi C_{12}\rho_1\rho_2}{12\Lambda^2} \tag{6}$$

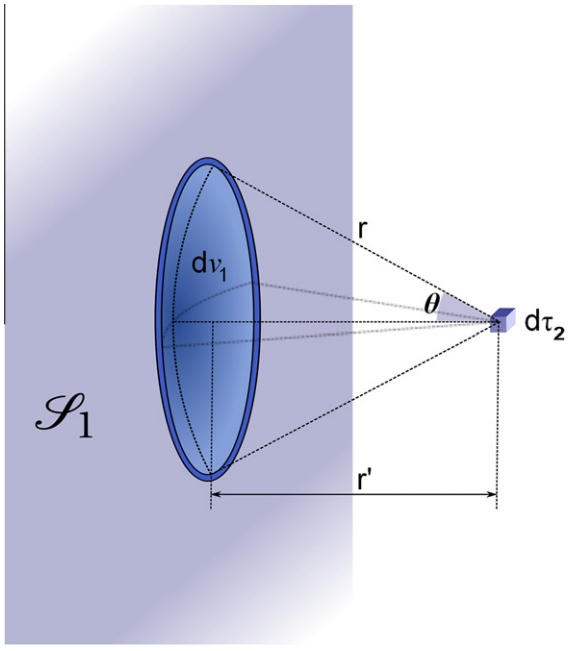

Fig. 1. Elementary volume $\mathrm{d}v_1$ from the half-space $\mathcal{S}_1$ interacting with $\mathrm{d}\tau_2$ from half-space $\mathcal{S}_2$.

To write the expression of the surface energy, let us consider that $\mathcal{S}_1$ and $\mathcal{S}_2$ are initially separated by an interatomic distance and finally by an infinite distance. The interatomic distance will now be referred to as a_0. We must not forget that this break does not form one but two new free surfaces. These couple of remarks justify the following expression of γ:

$$\gamma = \frac{W(\infty) - W(a_0)}{2} \tag{7}$$

Using Eq. (6) and noting that $W(\infty) = 0$, we get this new formula:

$$\gamma = \frac{A}{24\pi a_0^2} \tag{8}$$

where A is termed Hamaker constant. Its expression is given by:

$$A = \pi^2 C_{12} \rho_1 \rho_2 \tag{9}$$

The Eq. (8) form of γ will be the reference for further comparisons of surface energies. This expression was built so that it applies to ideal flat and smooth solid surfaces. However, we know that it is still valid to describe practical cases such as rough solid surfaces: the well known Wenzel's wetting equation (Wenzel, 1936) is still widely used today to predict the equilibrium contact angle of a liquid on a rough surface. This equation describes the increase of the real surface of the solid–liquid contact which leads to the reinforcement of the native hydrophobic or -philic behavior. But it does not assume any change of surface energy in the asperities. The observation of the γ expression shows that the only scale reference is the intermolecular distance a_0. Common surfaces have irregularities characterized by a large length compared to a_0 so that their effects remain imperceptible. How about nanotextured surfaces? Classical values of a_0 are about a few ångtröms so a more precise study is necessary for nanoscales.

5. Study of a full and isolated sphere

5.1. Potential energy expression

Let's consider the solid $\mathcal{S} = \{\mathcal{S}_1 \cup \mathcal{S}_2\}$ again but with a different split. $\mathcal{S}_1$ is a sphere with a radius R. $\mathcal{S}_2$ is a solid that fills all the universe but an empty spherical part centered on $\mathcal{S}_1$, with a radius $R + \Lambda > R$.

Let us study the potential energy linked to the interaction between a volume element $d\tau_2 \in \mathcal{S}_2$ and the sphere $\mathcal{S}_1$ with center $l \geqslant R + \Lambda$ away from $d\tau_2$. $\mathcal{S}_1$ is divided into volume elements dv_1 featured by a distance r from $d\tau_2$ (see Fig. 2).

The first difficulty is to determine the expression of dv_1 in terms of R, l and r. Volume element dv_1 is a spherical cap that is the intersection of $\mathcal{S}_1$ and a spherical surface with a radius r centred on $d\tau_2$ and which elementary thickness is noted dr (see Fig. 2).

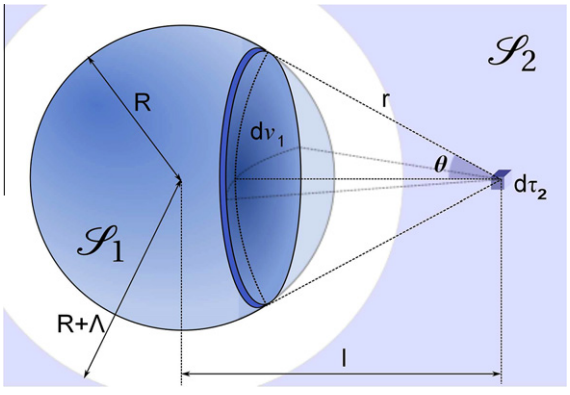

Fig. 2. Elementary volume dv_1 from the sphere $\mathcal{S}_1$ interacting with $d\tau_2$ from $\mathcal{S}_2$.

The current expression of dv_1 looks like the previous one. We use again Eq. (2). Basic geometry principles let us express $\cos\theta$ in terms of three lengths:

$$R^2 = l^2 + r^2 - 2lr\cos\theta \tag{10}$$

so that:

$$dv_1 = \pi \frac{r}{l}\left[R^2 - (l-r)^2\right]dr \tag{11}$$

Then, the distance r must be integrated over $\mathcal{S}_1$, that is from $l - R$ to $l + R$, as:

$$d\mathcal{E} = -d\tau_2 \frac{C\pi\rho_1\rho_2}{l}\int_{l-R}^{l+R} dr \frac{R^2 - (l-r)^2}{r^5} \tag{12}$$

$$d\mathcal{E} = -d\tau_2 \frac{C\pi\rho_1\rho_2}{l}\frac{1}{12}\left\{\frac{2R}{(l+R)^3} + \frac{2R}{(l-R)^3} + \frac{1}{(l+R)^2} - \frac{1}{(l-R)^2}\right\} \tag{13}$$

where $d\tau_2$ can be enlarged to a spherical cap that surrounds $\mathcal{S}_1$:

$$d\tau_2 = 4\pi l^2 dl \tag{14}$$

To finish with the potential energy expression, we must add every single $d\tau_2$ contribution over the entire $\mathcal{S}_2$ volume. The next formula gives the whole energy of the interaction between $\mathcal{S}_1$ and $\mathcal{S}_2$.

$$\mathcal{E} = -\frac{C\pi\rho_1\rho_2}{12}\int_{R+\Lambda}^{\infty} dl\, 4\pi l^2 \times \frac{1}{l}\left\{\frac{2R}{(l+R)^3} + \frac{2R}{(l-R)^3} + \frac{1}{(l+R)^2} - \frac{1}{(l-R)^2}\right\} \tag{15}$$

The primitive above vanishes at $+\infty$ so that the final expression is:

$$\mathcal{E} = -\frac{C\pi\rho_1\rho_2}{12} 4\pi\left\{\frac{2R(R+\Lambda)[R^2 + (R+\Lambda)^2]}{4R(R\Lambda^2 + \Lambda^3) + \Lambda^4} - \ln\left(\frac{2R+\Lambda}{\Lambda}\right)\right\} \tag{16}$$

5.2. Surface energy expression

The method used to get the flat surface energy is used again here. We first express the interaction energy per unit surface $W(\Lambda)$:

$$W(\Lambda) = \frac{\mathcal{E}}{4\pi R^2} \tag{17}$$

that is

$$W(\Lambda) = -\frac{C\pi\rho_1\rho_2}{12}\left\{\frac{(R+\Lambda)[R^2 + (R+\Lambda)^2]}{2R\Lambda^2\left(R + \frac{\Lambda}{2}\right)^2} - \frac{1}{R^2}\ln\left(\frac{2R+\Lambda}{\Lambda}\right)\right\} \tag{18}$$

and then, we can express surface energy $\gamma_S(R)$ of the sphere with Eq. (7)

$$\gamma_S(R) = \frac{A}{24\pi a_0^2}\left\{\frac{(R+a_0)[R^2 + (R+a_0)^2]}{2R\left(R + \frac{a_0}{2}\right)^2} - \frac{a_0^2}{R^2}\ln\left(\frac{2R+a_0}{a_0}\right)\right\} \tag{19}$$

$$\gamma_S(x) = \frac{A}{24\pi a_0^2}\left\{\frac{(x+1)[x^2 + (x+1)^2]}{2x\left(x + \frac{1}{2}\right)^2} - x^{-2}\ln(2x+1)\right\} \tag{20}$$

$$\gamma_S(x) \equiv \gamma \times \zeta(x) \tag{21}$$

One will recognize surface energy of a flat surface γ from Eq. (8). We defined a new function $\zeta(x)$ that is a correction factor that depends on R. All the problem reduces to this function. We introduced $x = R/a_0$ as the sphere radius value normalized to the mean intermolecular distance. We can equally use either R or x to define the sphere or any other quantity.

5.3. Asymptotic study: case of a high radius sphere

The goal of this part is to check whether the γ_S expression predicts that a little curved sphere behaves like a flat surface. In other words, we aim to investigate what happens to the $\zeta(x)$ value when x is much greater than 1. The two terms inside can first be approximated by:

$$\zeta(x >> 1) \sim \{1 - x^{-2} \ln 2x\} \tag{22}$$

which could be problematic. Fortunately, the limit is favorable

$$\lim_{x \to +\infty} x^{-2} \ln(2x) = 0 \tag{23}$$

and leads to

$$\zeta(x >> 1) = 1 \tag{24}$$

or, in terms of surface energy,

$$\gamma_S(x >> 1) = \gamma \tag{25}$$

which is the expected result. It wholly agrees with the assumptions, based on experience, we made previously concerning the imperceptible effect of solid surface imperfections on surface energy as long as these imperfections have high scales compared to the intermolecular distance of the matter.

5.4. Full study of the $\zeta(x)$ function

The $\zeta(x)$ function is plotted in Fig. 3. Its values are displayed against x from 1 up to 10^3 that is to say for R ranging from a_0 to $10^3 a_0$. First, one must notice that $\zeta(x)$ tends to reach unit value when the sphere radius gets high enough (as shown in the previous paragraph). Its behavior is more complex for low R values. It notably has a maximum for $R \approx 2\ a_0$. In this case, surface energy of the sphere is about 16% higher than for a flat surface (see Table 1). Second statement: the function is always greater than 1. This is one important result of this paper: a highly curved surface behaves more energetically than a flat one. This can be of great importance when dealing with nanoparticles. Indeed, a given volume of nanoparticles, apart from having a huge effective surface, has its surface energy intrinsically increased. This prediction concurs with Shimada's (Shimada et al., 1993) and Nanda's (Nanda et al., 2003) experimental works. They reported that the evaporation temperature of nanoparticles is strongly affected by their size. The smaller the particle, the lower the evaporation temperature (according to Kelvin's equation).

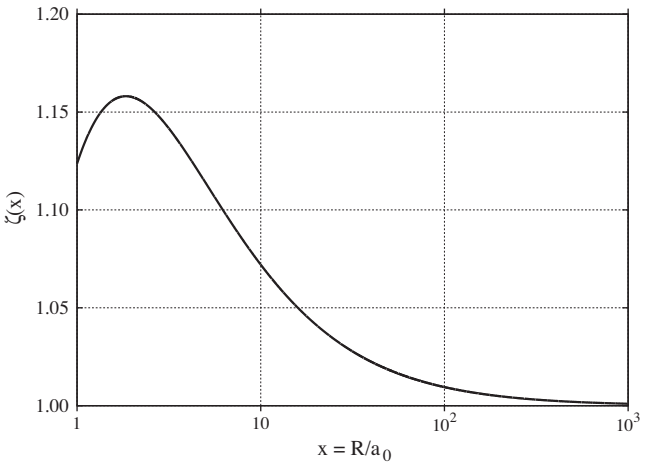

Fig. 3. Correction factor $\zeta(x)$ of the surface energy γ_S of a sphere to its nominal value γ for a flat surface – the graph is plotted against an x logarithmic scale.

Table 1
Radius of the sphere and percentage of over-energy at the surface for some x values – R is computed assuming an intermolecular distance a_0 = 3.5 Å.

x	R/nm	$(\zeta(x) - 1)$ Λ%
1	(a_0) 0.35	12.3
1.84	0.64	(maxi) 15.8
14.3	5.0	5.5
28.6	10	3.0
57.1	20	1.6
143	50	0.67
286	100	0.34
2860	1000	0.035

Another important result depicted by Fig. 3 is the decrease of the surface energy observed for $R < 2a_0$, that is more or less a free single particle. This decrease plays a stabilizing role concerning vapors. It must be favorable to the evaporation or the sublimation of a liquid or a solid respectively. Both the bulk and a single particle (case of vapors) are more stable than an aggregate of a few numbers of entities. Such a kind of small aggregates should either get bigger (crystal growth) or decay (evaporation) if the environment and the thermal agitation help. The maximum of energy on Fig. 3 can be interpreted as a sort of activation energy necessary to extract one atom from the surface. The energy is needed to go from the state "*surface atom*" to the state "*free atom*". For this reason, the activation energy is all the more weak than the mother-particle is small. It explains why the evaporation temperature decreases with the particle radius.

The function $\zeta(x)$ is plotted from $x = 1$, that is the minimum value with a physical meaning. The main reason of this choice is to let the reader have an idea of the hypothetical behavior of such an entity. Nonetheless, the 1 to 10 x-range does not seem to be a technologically reachable scale for nanotextured surface. Though, the field of nanoparticles could be largely affected by this extra energetic term as discussed above. In contrast to this, x values greater than 10 are more likely and really interesting for nanostructured surfaces. One can notice on Fig. 3 or in Table 1 that a few percent over-energetic term still remains while the scale is greater than 5 nm.

6. Sphere in a periodic environment

A nanometric entity seldom stands alone. Whether we deal with the asperities of a nanotextured surface or with free nanoparticles, we should take into account the proximity of a big number of them.

6.1. Expression of the surface energy

Let's consider that the sphere is not alone but constitutes one element of an infinite lattice of spheres. Note that, given the symmetry of all equations, this scheme can describe spherical asperities inside a solid as well as solid spheres in the vacuum. Center-to-center distance is $D = \Delta + 2R$ (see details on Fig. 4). What happens with $\mathcal{S}_1$ surface energy $\gamma_S(R)$? We will refer to this new effective surface energy as $\gamma_S^*(R, D)$. A rigorous expression will be developed in the next part. We can first check a simpler model. We will consider that $\mathcal{S}_1$ is surrounded by a homogeneous solid, with atomic density ρ, for radius ranging from $R + a_0$ up to $R + \Delta$. Beyond that, there is another solid, assumed to be homogeneous too, which atomic density is reduced. It is noted $[1 - \eta(R,D)]\rho$. The term $\eta(R,D)$ stands for solid porosity i.e. the ratio of empty volume to a given volume of the system.

$$\gamma_S^*(R,D) = \frac{1}{2}[W(\infty) - W(a_0)] - \frac{1}{2}\eta(R,D)[W(\infty) - W(\Delta)] \tag{26}$$

$$\gamma_S^*(R,D) = \gamma_S(R) + \frac{\eta(R,D)}{2} W(\Delta) \tag{27}$$

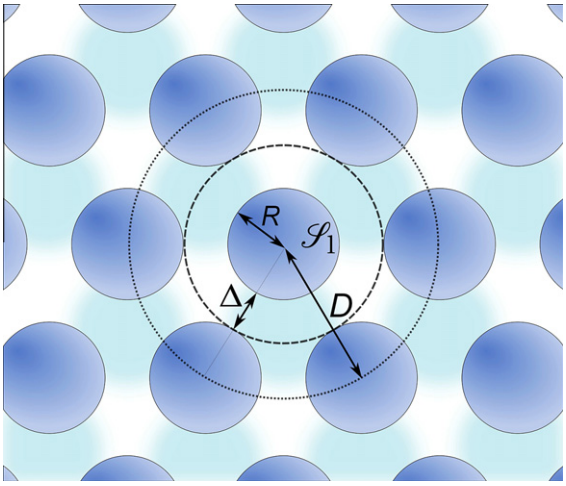

Fig. 4. Sphere $\mathcal{S}_1$ surrounded by a hexagonal lattice of clones – center-to-center distance is D. Free space between two spheres is $\Delta = D - 2R$.

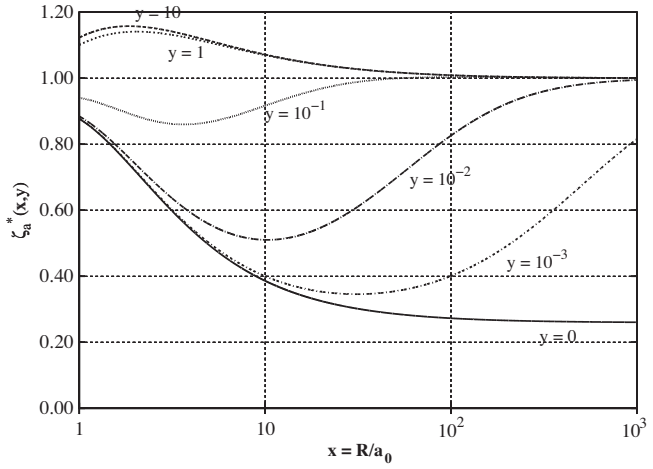

Fig. 5. Correction factor $\zeta^*(x,y)$ of the surface energy γ_S^* of a sphere in a periodic environment to its nominal value γ for a flat surface – the function was obtained with a simplified model assuming two homogeneous solids.

Again, we use reduced quantities and we define $y = (\Delta - a_0)/R$. The arbitrary choice to subtract a_0 from Δ is a comfort choice because, in this way, $y = 0$ is allowed and is associated to the smallest distance between two neighbors, which is a_0, regardless of R value. Porosity formula is based on the assumption of a hexagonal structure.

$$\eta(x,y) = \frac{\frac{4}{3}\pi R^3}{4\sqrt{2}\left(R+\frac{\Delta}{2}\right)^3} \tag{28}$$

$$\eta(x,y) = \frac{\pi}{3\sqrt{2}}\left(1+\frac{x^{-1}+y}{2}\right)^{-3} \tag{29}$$

Moreover, it can be shown that:

$$W(\Delta) = -\frac{A}{12\pi a_0^2}\frac{a_0^2}{\Delta^2}\left\{\frac{(R+\Delta)[R^2+(R+\Delta)^2]}{2R\left(R+\frac{\Delta}{2}\right)^2} - \frac{1}{R^2}\ln\left(\frac{2R+\Delta}{\Delta}\right)\right\} \tag{30}$$

$$W(\Delta) = -2\gamma\frac{a_0^2}{R^2}\frac{R^2}{\Delta^2}\zeta\left(\frac{R}{\Delta}\right) \tag{31}$$

$$W(x,y) = -2\gamma(1+xy)^{-2}\zeta\left((x^{-1}+y)^{-1}\right) \tag{32}$$

Now, the computation of $\gamma_S^*(x,y)$ can be reached using Eqs. (27) and (32):

$$\gamma_S^*(x,y) = \gamma\left[\zeta(x) - (1+xy)^{-2}\eta(x,y)\zeta[(x^{-1}+y)^{-1}]\right] \tag{33}$$

$$\gamma_S^*(x,y) \equiv \gamma \times \zeta_a^*(x,y) \tag{34}$$

We introduced $\zeta_a^*(x,y)$, the new correction factor to the surface energy for the sphere, surrounded by an hexagonal arrangement of its clone spheres. This factor is an approximation given by the simplified model. $\zeta_a^*(x,y)$ is plotted on Fig. 5 against x for six different representative y values.

The first criterium that must be checked is that $\zeta_a^*(x,y)$ should look like $\zeta(x)$ when y is high enough. Fig. 5 clearly shows this similarity, even for $y = 10$, that's to say $\Delta \approx 10R$ (exact if $R >> a_0$). For such a y value, the nearest neighbors spheres are so far that they do not interact with each other.

The effective porosity of the solid tends to decrease effective surface energy of the sphere. This element is opposed to the intrinsic over-energy observed for high curvatures (small radii). The lower the y value, the more important the x-range that porosity acts on. The ultimate case, $y = 0$ concerns spheres in intimate contact ($\Delta = a_0$). The dedicated curve on Fig. 5 shows that $\zeta_a^*(\infty,0)$ tends to 0.26. One must observe that $0.26 = 1 - 0.74$ where 0.74 is the known classical packing efficiency of a hexagonal close-packed structure.

This last result is in agreement with current model concessions we made and shows that the model behaves the way it was built. However, it also constitutes the proof that this model is only valid for high y values. As expected, when the spheres are too close, the assumption of an equivalent homogeneous solid fails and leads to a bad prediction. Indeed, when the cavities (or the spheres) are in intimate contact, solid (or vacuum) situated around tetrahedral sites is still there and wholly plays its role in van der Waals potential expression. A good model should predict $\zeta_a^*(\infty,0) = 1$.

6.2. Rigorous computation of surface energy

A more accurate model implies the knowledge of the energy of two interacting spheres. This energy must be subtracted from $\gamma_S(R)$. Hamaker carried out this calculation (Hamaker, 1937). He showed that two spheres of same radius R and with a distance d between their centers have a potential energy of interaction:

$$\mathcal{E} = -\frac{A}{6}\left\{\frac{2R^2}{d^2-4R^2} + \frac{2R^2}{d^2} + \ln\frac{d^2-4R^2}{d^2}\right\} \tag{35}$$

Assuming a hexagonal close-packed structure, we can express the three basic vectors of the lattice **a**, **b** and **c** in terms of unitary vectors of an orthonormal basis **i**, **j** and **k**:

$$\mathbf{a} = D\mathbf{i} \tag{36}$$

$$\mathbf{b} = \frac{D}{2}\mathbf{i} + \frac{D\sqrt{3}}{2}\mathbf{j} \tag{37}$$

$$\mathbf{c} = \frac{D}{2}\mathbf{i} + \frac{D}{2\sqrt{3}}\mathbf{j} + \sqrt{\frac{2}{3}}D\mathbf{k} \tag{38}$$

Let **X** be the representative vector of an entity belonging to the hexagonal lattice. Its generic expression is:

$$\mathbf{X} = m\,\mathbf{a} + n\mathbf{b} + p\mathbf{c} \quad (m,n,p) \in \mathbb{N}^3 \tag{39}$$

Its distance d to the original sphere is:

$$d^2 \equiv \|\mathbf{X}\|^2 = D^2[(m+n+p)^2 - (mn+mp+np)] \tag{40}$$

In other words, the center-to-center distance between any spheres can be expressed as:

$$d_i = \lambda_i D \tag{41}$$

where λ_i is a factor such as:

$$\lambda_i = \sqrt{(m+n+p)^2 - (mn+mp+np)} \tag{42}$$

$$\lambda_i = \sqrt{i} \quad i \in \mathbb{N}^{*+} \tag{43}$$

The main problem is knowing how many different **X** vectors are associated with the same λ_i value. This is not trivial! On the other hand, it is quite easy to program an algorithm that tries every combination (m,n,p) and saves its contribution. Table 2 gives n_i, the λ_i-degeneracy, for the 10 smallest distances.

The energy, per unit surface, associated with the interaction of two spheres separated by a distance D (reference) is (Hamaker, 1937):

$$W = \frac{\mathcal{E}}{8\pi R^2} \tag{44}$$

$$= -\frac{A}{24\pi}\left\{\frac{1}{D^2-4R^2} + \frac{1}{D^2} + \frac{1}{2R^2}\ln\frac{D^2-4R^2}{D^2}\right\} \tag{45}$$

$$W = -\gamma\left\{\frac{1}{(xy+2x+1)^2-4x^2} + \frac{1}{(xy+2x+1)^2} + \frac{1}{2x^2}\ln\frac{(xy+2x+1)^2-4x^2}{(xy+2x+1)^2}\right\} \tag{46}$$

So, taking into account all possible distances d_i and all actors for each distance, the surface energy of the sphere in its hexagonal lattice is:

$$\gamma_S^*(x,y) = \gamma\zeta(x) - \gamma\sum_{i=1}^{\infty} n_i\left\{\frac{1}{\lambda_i^2(xy+2x+1)^2-4x^2} + \frac{1}{\lambda_i^2(xy+2x+1)^2} + \frac{1}{2x^2}\ln\frac{\lambda_i^2(xy+2x+1)^2-4x^2}{\lambda_i^2(xy+2x+1)^2}\right\} \tag{47}$$

$$\gamma_S^*(x,y) \equiv \gamma \times \zeta^*(x,y) \tag{48}$$

The rigorous correction factor $\zeta^*(x,y)$ is defined. It replaces the approximated correction factor $\zeta_a^*(x,y)$ of the last paragraph. Let's take a look at the plot of this new more realistic function (see Fig. 6) so that we can compare it with the previous one (Fig. 5). Note that Fig. 6 uses Eq. (47) with the only four first distances $\left(\sum_{i=1}^{4}\right)$, which gives a very good numeric approximation.

Looking at the graph of Fig. 6 gives us several evidences of the coherence of this new model with the previous one. First, it seems that an increase of y – reflecting a large distance between the spheres – makes $\zeta^*(x,y)$ tend to $\zeta_a^*(x,y)$ (and so to $\zeta(x)$). In a more general way, we can see that the simple model gives good predictions as long as y is greater than 0.5. Below this value, the simple model deteriorates and is no longer able to make proper predictions. In fact, the region surrounding the sphere, closer than a half sphere-radius has too much impact through van der Waals potential to be approximated by a homogeneous less dense medium: the rigorous model is to be used below this limit. Secondly, we have fixed the bad behavior of the correction factor when y tends to 0. This time, $\zeta^*(x,0)$ no longer tends to 0.26 but to 1. In other words, even though spheres are in intimate contact ($\Delta = a_0$), a big radius R makes it so that tetrahedral sites are dominant around the sphere and cancel any proximity effect.

Table 2
Number n_i of neighbors found at a distance $d_i = \lambda_i D$ of the sphere.

i	1	2	3	4	5	6	7	8	9	10	...
λ_i	1	$\sqrt{2}$	$\sqrt{3}$	2	$\sqrt{5}$	$\sqrt{6}$	$\sqrt{7}$	$2\sqrt{2}$	3	$\sqrt{10}$	...
n_i	12	6	24	12	24	8	48	6	36	24	...

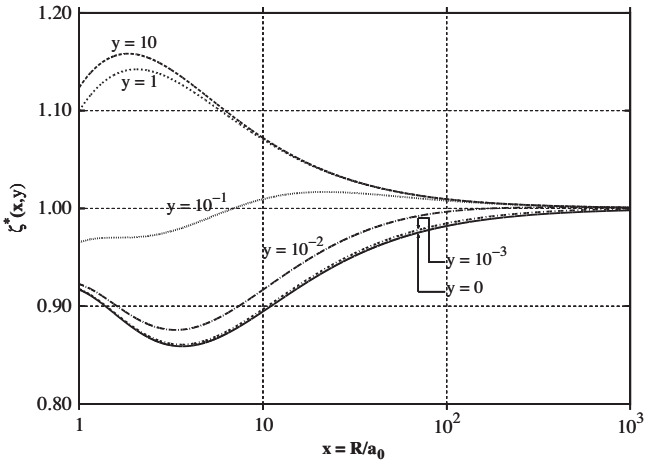

Fig. 6. Correction factor $\zeta^*(x,y)$ of the surface energy γ_S^* of a sphere in a periodic environment to its nominal value γ for a flat surface – the function was obtained with a rigorous model assuming each sphere-sphere interaction.

In a more general way, and as expected, the new function $\zeta^*(x,y)$ reveals a much less strong effect of the porosity on the surface energy. Even the more favorable case in terms of surface energy loss ($x \sim 4$) hardly shows a decrease of 15%. However, this effect is not negligible and should be reported and accounted when dealing with compacted nanopowders which typical radii are lower than about 30 or 40 nm ($x \sim 10^2$ on the graph).

These results also concur with numerous studies on that the energy of a single-crystal surface strongly depends on its Miller's index. It was experimentally pointed out that the higher Miller's index, the less filled is the plane and, as a result, the higher is the surface energy. Jia et al. (2009) mention a difference of 10% between surface energies of [110] and [100] faces of fcc copper nanoparticles. Although these sorts of crystal planes are not in the scope of this study, our model (Fig. 6) qualitatively predicts the variations of energy with the particle neighborhood (y value). An isolated single particle ($x = 1, y >> 1$) has an energy 20%-larger than the same one close to 12 neighbors ($x = 1, y = 0$). The factor 2 between Jia's predictions and ours can be partly explained by that Jia always assumes surface atoms in contact with a full half-space (the bulk).

7. Conclusions

The van der Waals potential was integrated over planar and spherical bodies. It was clearly shown that the surface energy is dependent on the curvature, particularly when the radius is lower than 100 intermolecular distances. This dependence consists of an over-energetic term which is in contrast with Tolman's prediction but is confirmed by experiments based on evaporation of Ag nanoparticles. The proximity of other nano-entities, whether we focus on nanoparticles or nanostructuration in a solid bulk, was also theoretically investigated. Two models were used. On the one hand, a simple model, based on a homogeneous less dense surrounding medium, is not applicable when entities are closer than a half sphere-radius. On the other hand, a second model, based on rigorous computation of interactions between the sphere and its closest neighbors, gave more valuable information. It showed that the nano-porosity of a solid or a compact group of nanoparticles both lead to a substantial decrease of surface energy as long as the radius of curvature is less than 30 or 40 nm. A maximum of 15% decrease is predicted for 2 or 3 nm. Above 30 nm, the surface energy tends to reach its classical value. We believe these results, although based on the case of spheres, can be extended to all types of nanostructured surfaces. They could help to achieve a better understanding of the behavior of nanoporous surfaces.

References

Awitor, K., Rafqah, S., Géranton, G., Sibaud, Y., Larson, P., Bokalawela, R., Jernigen, J., Johnson, M., 2008. Journal of Photochemistry and Photobiology A: Chemistry 199, 250–254.

Aw, M., Simovic, S., Addai-Mensah, J., Losic, D., 2011. J. Mater. Chem..

Bradley, R., 1932. Philosophical Magazine 13, 853.

Baidakov, V., Boltachev, G., 1999. Physical Review E 59, 469.

De Boer, J., 1936. Transactions of the Faraday Society 32, 10–37.

Derjaguin, B.V., 1934. Colloid and Polymer Science 69, 155–164.

Fisher, M., Wortis, M., 1984. Physical Review B 29, 6252.

Guermeur, R., Biquard, F., Jacolin, C., 1985. The Journal of Chemical Physics 82, 2040.

Gultepe, E., Nagesha, D., Sridhar, S., Amiji, M., 2010. Advanced Drug Delivery Reviews 62, 305–315.

Hamaker, H., 1937. Physica 4, 1058–1072.

Hill, T.L., 1950. Journal of the American Chemical Society 72, 3923–3927.

Jia, M., Lai, Y., Tian, Z., Liu, Y., 2009. Modelling and Simulation in Materials Science and Engineering 17, 015006.

Kwak, D., Yoo, J., Kim, D., 2010. Journal of Nanoscience and Nanotechnology 10, 345–348.

Lei, Y., Bykov, T., Yoo, S., Zeng, X., 2005. Journal of the American Chemical Society 127, 15346–15347.

Liang, Y., Cui, Z., Zhu, S., Yang, X., 2011. Journal of Materials Science: Materials in Medicine, 1–7.

Moody, M., Attard, P., 2001. The Journal of Chemical Physics 115, 8967.

Nishioka, K., Tomino, H., Kusaka, I., Takai, T., 1989. Physical Review A 39, 772–782.

Nanda, K., Maisels, A., Kruis, F., Fissan, H., Stappert, S., 2003. Physical Review Letters 91, 106102.

Nanda, K., 2005. Applied Physics Letters 87, 021909.

Park, J., Bauer, S., von der Mark, K., Schmuki, P., 2007. Nano Letters 7, 1686–1691.

Perry, J., Martin, C., Stewart, J., 2011. Chemistry – A European Journal 17, 6296–6302.

Robert-Goumet, C., Monier, G., Zefack, B., Chelda, S., Bideux, L., Gruzza, B., Awitor, O., 2009. Surface Science 603, 2923–2927.

Shimada, M., Seto, T., Okuyama, K., 1993. AIChE Journal 39, 1859–1869.

Tolman, R., 1948. The Journal of Chemical Physics 16, 758.

Van Giessen, A., Blokhuis, E., Bukman, D., 1998. The Journal of Chemical Physics 108, 1148.

von Wilmowsky, C., Bauer, S., Roedl, S., Neukam, F.W., Schmuki, P., Schlegel, K.A., 2011. Clinical Oral Implants Research.

Wenzel, 1936. Industrial and Engineering Chemistry, 988.

Y. Yang, K. Leong, Wiley Interdisciplinary Reviews: Nanomedicine and Nanobiotechnology, 2010.